I&EC research
Industrial & Engineering Chemistry Research

Article

pubs.acs.org/IECR

Acceleration of Kinetic Monte Carlo Method for the Simulation of Free Radical Copolymerization through Scaling

Hanyu Gao,[†] Lindsay H. Oakley,[‖] Ivan A. Konstantinov,[‡] Steven G. Arturo,[§] and Linda J. Broadbelt*[,†]

[†]Department of Chemical and Biological Engineering, Northwestern University, 2145 Sheridan Road, Evanston, Illinois 60208, United States

[‡]The Dow Chemical Company, 2301 North Brazosport Blvd., Freeport, Texas 77541, United States

[§]The Dow Chemical Company, 400 Arcola Road, Collegeville, Pennsylvania 19426, United States

[‖]Department of Materials Science and Engineering, Northwestern University, 2220 Campus Drive, Evanston, Illinois 60208, United States

Supporting Information

ABSTRACT: Kinetic Monte Carlo (KMC) has become a well-established technique for simulating the kinetics of free radical polymerization, both to generate polymer molecular weight distributions and, more recently, to track the explicit monomer sequence in every chain. However, KMC simulations require a minimal number of molecules in order to accurately describe monomer conversion and macromolecular quantities, which can render them computationally prohibitive. In this work, we propose a novel approach for accelerating KMC simulations through scaling relationships that allow the number of molecules simulated to be reduced. Using the concept of the minimal number of molecules and an explicit expression we derived for copolymerization, we propose a factor that is used to scale the reaction rate constants which results in an acceleration of KMC simulations by a factor of ∼100. Furthermore, we demonstrate the limits of this scaling approach, revealing the absolute lower bound for the number of molecules used in KMC simulations of free radical polymerization and the associated population size of dead chains formed. We illustrate this approach using examples of acrylate copolymerization, but this approach is sufficiently general that it can be applied to a wide variety of free radical polymerization systems and even other free radical chemistries.

1. INTRODUCTION

Kinetic Monte Carlo (KMC) employing the Gillespie algorithm has been used to simulate chemical reactions for the past 40 years.[1] The method takes into account the stochastic nature of the chemical reactions by randomly sampling reaction events based on their relative rates. One field where KMC has demonstrated its advantage over deterministic approaches is free radical polymerization. The ability to track the explicit sequence of the individual chains during polymerization has proven crucial to understanding the physical and chemical properties of the polymer products.[2−6]

A growing number of studies have applied KMC to study polymerization reactions.[7−26] For example, Meimaroglou and Kiparissides[9] developed a KMC model combined with molecular modeling to predict the rheological properties and topological characteristics of highly branched polymers. Sosnowski[10] developed software for free radical and living radical polymerization based on KMC. Mohammadi et al.[20] used a KMC method to study free radical polymerization of branched copolymers, with a focus on the effect of reactivity ratio and initial feed composition. Chaffey-Millar et al.[23] improved the efficiency of the KMC algorithm by using binary trees to store and retrieve the chain lengths and reaction rates. Van Steenberge et al.[11] improved the KMC algorithm for simulating the chemical composition−chain length distributions of polymerization processes. Regatte et al.[12] developed a KMC model to predict synthesis recipes to achieve sequence and molecular weight targets of copolymers. Recently, Tripathi and Sundberg[13] demonstrated a hybrid simulation method in which propagation events are treated continuously while initiation and termination events are treated stochastically, which significantly reduced simulation time. A recent and comprehensive review by Brandão et al.[22] describes related rapid developments in the field of KMC simulations applied to polymer reaction engineering.

Despite the advantage of modeling explicit sequences, a major drawback of KMC is the intrinsic computational demand. This is primarily due to the large number of molecules and subsequent reaction events in the system. In this context, we define the "system size" as the total number of initial molecules used in KMC simulations. The number of reaction events is a linear function of the system size which, if reduced, would decrease the simulation time. As expected with stochastic models, the system size has a lower bound. In multiple studies,[14,16−19] researchers have identified the minimal system size required to obtain converged results, e.g., conversion and number and weight-average molecular weight.

In the context of the work described here, lack of convergence refers to the fact that the quantities of interest are still changing as the system size increases. This is different than convergence that is typically referred to in stochastic

Received: August 30, 2015
Revised: October 19, 2015
Accepted: October 26, 2015
Published: October 26, 2015

DOI: 10.1021/acs.iecr.5b03198
Ind. Eng. Chem. Res. 2015, 54, 11975−11985

simulations of, for example, thermodynamic properties,[27−29] where results from simulations of various numbers of molecules have the same average values but greater individual variation as the system size is decreased. In KMC simulations of free radical polymerization, repeated runs for a given system size provide the same outcome, but if the system size is too small, the result is different than the converged result. For a simulation of free radical polymerization with a system size smaller than the minimum, the Gillespie algorithm results in lower conversion than the true value. The deviation from the true value can be very large, and it is much larger than the small fluctuations that result from the stochastic nature of the simulation. As the system size approaches the minimum size necessary for convergence, conversion and molecular weight values are close to the correct values. Ultimately, convergence is found when systems of different sizes produce the same result. In most studies, this lower bound, typically between 10^6 and 10^{12} initial molecules, is determined at the beginning of the study. Subsequent runs at or larger than the lower bound are regarded as converged, regardless if the synthesis conditions (e.g., temperature, initiator concentration) that are being simulated are altered. Parsa et al.[30] reported this limit is related to the fact that the number of radicals, which is a dilute species in a free radical system, needs to be greater than or equal to two. They derived a general formula based on the pseudo-steady-state assumption (PSSA) that calculates the minimal control volume (proportional to the system size in this context) for homopolymerization. This result was applied by Tripathi and Sundberg in the development of their hybrid algorithm.[13] We expand on this concept for copolymerization and derive a relationship between minimal number of molecules and the parameters and reaction conditions governing the system.

On the basis of our understanding of the nature of this minimal system size, we introduce a method that demonstrates that mathematical scaling involving the rate constants allows the system size to be reduced while still preserving accurate results, thereby providing the ability to accelerate simulations.

This paper is organized as follows. First, the formula for calculating the minimal system size is derived in terms of number of molecules instead of control volume to facilitate later discussion. It is shown that the generalization of this formula for copolymerization and other more complicated free radical systems is possible, albeit not trivial, with proper assumptions. Next, the main body of the paper focuses on explaining the results when the system contains fewer than the minimum number of species and introduces a novel approach of scaling the rate coefficients with the ultimate goal of accelerating the KMC methodology. The scaling concept is demonstrated with several case studies.

2. BACKGROUND

2.1. Kinetic Monte Carlo Algorithm. The KMC method implemented here is based on the algorithm proposed by Gillespie.[1] The approach repetitively generates two random numbers to simulate chemical reactions stochastically.

The first random number is used to determine the time step between reaction events, denoted as τ. This is calculated by

$$\tau = \left(\frac{1}{a_0}\right)\ln(1/\mathrm{rn}_1) \tag{1}$$

where a_0 is the total rate defined as $a_0 = \sum_{\nu=1}^{m} R_\nu$ and rn_1 is a random number generated with a uniform distribution between 0 and 1. R_ν is the stochastic rate of the νth reaction channel.

The second random number determines which reaction occurs at the given instant, based on the reaction probabilities:

$$\sum_{\nu=1}^{\mu-1} P_\nu < \mathrm{rn}_2 \le \sum_{\nu=1}^{\mu} P_\nu \tag{2}$$

Where rn_2 is a random number uniformly distributed between 0 and 1, μ the index of the selected reaction channel, and P_ν the probability of the νth reaction channel, which is obtained based on its fraction of the total reaction rate as

$$P_\nu = \frac{R_\nu}{\sum_{\nu=1}^{m} R_\nu} \tag{3}$$

In a KMC simulation, these two random numbers are generated repetitively until the desired reaction time is reached. Further details of the KMC method can be found elsewhere.[16,31]

2.2. Free Radical Polymerization of Copolymers Described by a Penultimate Model. Free radical polymerization (FRP) of two different monomers has a wide range of applications in industry to produce different varieties of polymeric materials.[32] Typically, polymerization starts with the decomposition of initiator molecules to form radicals. Then the monomers successively add to the radical to form long-chain radicals. Two radicals terminate via recombination and/or disproportionation.

A penultimate model takes into consideration the effect that the penultimate unit has on the propagation and termination kinetics. This is shown to be important in many free radical polymerization systems.[33−35] In this work, we use the penultimate model for FRP that is the same as that used by Regatte et al.,[12] with a complete summary of the reaction mechanism given in Table 1.

3. METHODOLOGY

3.1. Calculating the Minimal System Size for Radical Reaction Systems. As previously discussed, the minimal

Table 1. Free Radical Polymerization Steps Incorporated into the Models in This Work[a]

reaction events	
initiation	
initiator decomposition	$I_2 \rightarrow 2I^\bullet$
chain initiation	$I^\bullet + M_i \rightarrow P_i^{\bullet(1)}$
propagation	
first propagation	$P_i^{\bullet(1)} + M_j \rightarrow P_{ij}^{\bullet(2)}$
penultimate effect	$P_{ij}^{\bullet(x)} + M_k \rightarrow P_{jk}^{\bullet(x+1)}$
termination	
by recombination	$P_{ij}^{\bullet(x)} + P_{jk}^{\bullet(y)} \rightarrow P^{(x+y)}$
by disproportionation	$P_{ij}^{\bullet(x)} + P_{jk}^{\bullet(y)} \rightarrow P^{(x)} + P^{(y)}$

[a] I_2 denotes initiator. $I^\bullet$ represents initiator radical. M_i represents monomer i. $P_i^{\bullet(1)}$ is a polymeric radical of chain length 1. $P_{jk}^{\bullet(x+1)}$ is a polymeric radical with penultimate unit of monomer j, a terminal unit of monomer k, and a total number of monomers of chain length $x + 1$. $P^{(x)}$ is a dead polymer chain of length x.

DOI: 10.1021/acs.iecr.5b03198
Ind. Eng. Chem. Res. 2015, 54, 11975−11985

system size must be determined in order to ensure that converged behavior is obtained so that the proper results are found. It has been reported in the literature[13,30] that the key question is to identify the system size that on average contains at least two radicals.

The relation between system size and the radical content for homopolymerization is built by applying PSSA, which assumes that the net rate of formation of radicals is zero. Because the propagation reactions do not change the number of radicals, radicals are formed only from initiation and consumed only through termination. Therefore, the rate of initiation should be equal to the rate of termination. Although there are circumstances in which assuming pseudo-steady state for radical concentration causes errors,[36−39] PSSA has been demonstrated to be a reasonable assumption for a wide range of radical polymerization systems.[40−43] For free radical polymerization, PSSA takes the form

$$k_i \times C_i = k_t \times C_r^2 \tag{4}$$

where k_i is the continuum initiation rate constant, C_i the concentration of initiator, k_t the continuum termination rate constant, and C_r the number of radicals. Note that

$$C_r = \frac{N_r}{N_A V} \tag{5}$$

where N_r is the number of radicals and V is the system volume. In this work, we adopt the convention of Szymanski[44] and do not multiply by a factor of 2 for radical termination equations.

The system volume can be related to the system size via the concentrations, mole fractions, and molar densities of all species as follows:

$$VN_A = N_{tot} \sum_{i \in \text{monomers,solvent}} \frac{x_j}{\rho_j} \tag{6}$$

where N_{tot} is the system size; x_j represents the mole fractions of monomers and the solvent, and ρ_j's are the molar densities of monomers and the solvent.

By substituting eqs 5 and 6 into eq 4, we obtain N_{tot} as a direct function of the number of radicals existing in the system. The number of radicals is set to two, and we obtain

$$N_{tot,min} = 2\sqrt{\frac{k_t}{k_i C_i}}\left(\sum_{j \in \text{all species}} \frac{x_j}{\rho_j}\right)^{-1} \tag{7a}$$

This formula is essentially the same as eqs 9 and 10 in ref 30 and eq 25 in ref 13, except that it is derived in the form of number of molecules here.

An important discussion at this point in the method development is why the stochastic rate expression for bimolecular reactions involving the same species, $R = (2k/VN_A)\cdot[N(N-1)/2]$, is not used in the derivation above, especially when it yields significant differences for termination from the continuum model value when the number of radicals is small. To establish PSSA, at least a certain period of time (e.g., a number of radical lifetimes) is needed, and the reaction rate is essentially a temporal *average*. The stochastic rate, however, is an *instantaneous* rate, and fluctuates with the number of radicals in the system. If one were to establish PSSA using the stochastic formulation, the formula is

$$k_i \times N_i = \overline{R_t} = \overline{\frac{2k_t}{VN_A} \times \frac{N_r(N_r - 1)}{2}} \tag{8}$$

where N_i is the number of initiator molecules and $\overline{R_t}$ represents the temporal average value of the stochastic termination rate. To determine the average number of radicals using eq 8 is difficult, because to evaluate the right-hand side one would need to know the distribution of number of radicals, i.e., how often the system contains zero radicals, two radicals, four radicals, etc. However, this distribution cannot be known prior to running the simulation. Therefore, eq 8 has little practical value in determining some quantities (e.g., minimal system size) before actual simulations are carried out. On the other hand, the continuum model provides a concise way of relating reaction rates to species concentrations and hence is used in this work for theory development and obtaining analytical solutions. More importantly, the theory developed using continuum expressions is valid and can be demonstrated as such in the context of stochastic simulations. We will show by example below that KMC simulations calculate a temporal average termination rate that is proportional to the square of the number of radicals. Also, it is important to point out that, in this work, the continuum rate expression is used only to derive the equations that calculate the minimal system size as well as the scale factor that will be introduced below. In the actual KMC simulations, the stochastic rates are used, and PSSA is not employed. However, we acknowledge that if certain cases for which PSSA was not valid were modeled, then the application of the scale factor would be restricted.

Equation 7a can be generalized for copolymerization. For copolymerization, the termination rate constant is a collective value for different homotermination and cross-termination reactions. The closed form of the effective termination rate constant can be rigorously derived as a combination of all different types of termination, which will be introduced in the next section. This complicates the form of the equation. However, researchers are often interested in obtaining only a rough estimate of the minimal system size to be used in KMC simulations. For this purpose, we may substitute the effective termination rate constant with the largest termination rate constant. This gives an upper bound for the system size which ensures the convergence of the KMC algorithm while still being reasonably close to the exact minimal system size.

$$N_{tot,min} \le 2\sqrt{\frac{k_{t,max}}{k_i C_i}}\left(\sum_{j \in \text{monomers,solvent}} \frac{x_j}{\text{dens}_j}\right)^{-1} \tag{7b}$$

Though eq 7b provides a convenient way to calculate an upper bound for the minimal system size, it requires a recalculation of the upper bound for each new simulation. Most studies run multiple KMC simulations for a certain range of operating conditions. It would be helpful to determine a universal upper bound that is valid for the whole range of synthesis conditions of interest. This can be achieved by using the minimal initiator concentration ($C_{i,min}$), the minimal temperature, and the maximum molar density for all species, resulting in the formula below:

$$N_{tot,min} \le 2\rho_{max}\sqrt{\frac{k_{t,max}(T = T_{min})}{k_i(T = T_{min})C_{i,min}}} \tag{7c}$$

DOI: 10.1021/acs.iecr.5b03198
Ind. Eng. Chem. Res. 2015, 54, 11975−11985

Note that in this formula all the parameters are known prior to running the simulations. With this universal upper bound, only one simple calculation is needed to determine a system size that ensures KMC convergence.

The scope of eq 7a can be further extended to more complicated radical reaction systems. To this end, we show an example of the autoxidative polymerization of alkyd paint systems. While the reaction mechanism is more complicated, it is also composed of initiation, propagation, and termination steps.[45] The model system involves technical grade ethyl linoleate (EL), a cobalt catalyst (cobalt ethyl hexanoate), and molecular oxygen.[46] Technical grade EL is about 65% pure, and most of the impurity is ethyl oleate which is much less reactive than EL and, consequently, treated as inert solvent. The reaction mechanism[46−48] can be found in the Supporting Information.

The number of elementary steps and species involved in this mechanism can quickly escalate to tens of thousands. Application of a KMC model framework allows each of these unique chemical species to be tracked explicitly and sequence information for the polymeric constituents to be stored. It facilitates access to more detailed information, allowing deeper insights and new conclusions to be made. Similarly to FRP, there is also a minimal system size requirement on this reaction network which needs to be determined before running the simulations.

By applying the PSSA to this system, we obtained the same result as the FRP case, i.e., the rate of initiation equals the rate of termination. For this case, however, initiation is more complicated; there are multiple channels, and some are more difficult to handle analytically. For example, the hydroperoxide decomposition reactions can be treated as initiation reactions because they create radicals. However, some of these reactions are highly coupled and the corresponding concentrations are difficult to determine. This makes the analysis of the effective rate of initiation quite complex. However, using eq 7a, it can be shown that by substituting the rate of initiation by a smaller number, a safe and computationally reasonable overestimation of the minimal system size can be obtained. This means that it is possible to neglect some of the initiation reaction channels while focusing on the most important ones. Once hydroperoxide decomposition reactions are excluded, an equation similar to eq 7a can be derived as follows:

$$N_{\mathrm{tot,min}} = 2\sqrt{\frac{k_{\mathrm{t,max}}}{k_{\mathrm{i}} C_{\mathrm{Co}} C_{\mathrm{O_2}}}}\left(\sum_{j\in \text{all species}} \frac{x_j}{\rho_j}\right)^{-1} \tag{7d}$$

where C_{Co} is the concentration of cobalt catalyst and $C_{\mathrm{O_2}}$ is the concentration of molecular oxygen.

3.2. Acceleration of KMC Simulations through Scaling. Although eq 7a and its generalized forms can be used to conveniently determine the minimal system size for radical reaction systems, the calculated minimal system size is usually still on the order of 10^8−10^9, which remains a major barrier for the efficient application of KMC algorithms. However, we can use the understanding of the origin of the minimal system size to develop a scaling approach to accelerate KMC simulations.

The deviation of the simulation results below the minimal system size is related to the fact that the number of radicals in a KMC simulation must be discrete. Normally, both the number of radicals and number of monomers existing in the system scales linearly with the system size. When reducing the system size, a point will be reached when the average number of radicals at a particular time is two (not one because according to our scheme, initiation reactions always generate radicals in pairs, but the derivation can be generalized to cases in which only one of the two radicals adds monomer). If the system size is reduced further, the number of monomers and the system volume will decrease proportionally, as the number of monomer molecules is still abundant. However, at the instant of an initiation event, the number of radicals generated is still two. This results in an increase in the radical concentration and affects all the reactions whose rates depend on radical concentration.

In this particular FRP mechanism, the reactions whose rates are dependent on the radical concentration include propagation and termination, which can be seen from the rate expressions (continuum formulation)

$$r_{\mathrm{i}} = k_{\mathrm{i}} \times C_{\mathrm{i}} = k_{\mathrm{i}} \times \frac{N_{\mathrm{i}}}{VN_{\mathrm{A}}} \tag{9}$$

$$r_{\mathrm{p}} = k_{\mathrm{p}} \times C_{\mathrm{r}} \times C_{\mathrm{m}} = k_{\mathrm{p}} \times \frac{N_{\mathrm{r}} \times N_{\mathrm{m}}}{(VN_{\mathrm{A}})^2} \tag{10}$$

$$r_{\mathrm{t}} = k_{\mathrm{t}} \times C_{\mathrm{r}}^2 = k_{\mathrm{t}} \times \left(\frac{N_{\mathrm{r}}}{VN_{\mathrm{A}}}\right)^2 \tag{11}$$

where r_{i}, r_{p}. and r_{t} are the continuum rates of initiation, propagation, and termination, respectively. A lower case letter is used to differentiate the continuum rate formulation from the stochastic ones. k_{i}, k_{p} and k_{t} are the rate constants for initiation, propagation and termination, respectively. C_{m} is monomer concentration, and N_{m} is the number of monomer molecules.

When the system size becomes too small, the termination-to-propagation rate ratio increases. This grants the radicals a higher tendency to terminate than propagate. Consequently, the chains become shorter, and a lower average molecular weight is observed. In addition, propagation cannot take place until another initiation event occurs. In a macroscopic system, propagation would occur between initiation events, consuming monomer and increasing conversion. This explains why with an insufficient number of molecules, lower conversion is observed compared to a macroscopic system.

On the basis of the analyses above, we have proposed a method that enables us to reduce the system size below the calculated minimum described by eq 7b. We will show that converged results can be maintained, provided that proper mathematical scaling is applied to the relevant rate constants. In addition to accelerating the simulation, this novel approach further reduces the system size and has the additional important application of potentially linking KMC simulations to molecular simulations. KMC simulations generate explicit chain information. This sequence information can be used for molecular simulations to model the physical and chemical properties of the polymeric product. However, the chain population created by a typical KMC simulation is typically too large and cannot be accommodated by molecular simulations. The new method creates a smaller chain population that shares the same properties (e.g., molecular weight distribution, distribution of dyads, triads, tetrads, etc.) as the one obtained from a larger system size.

Our approach focuses on maintaining the correct rates even when radical concentration rises, by scaling the rate constants

DOI: 10.1021/acs.iecr.5b03198
Ind. Eng. Chem. Res. 2015, 54, 11975−11985

of all reactions that depend on the radical concentration. All rates that depend on radical concentration to the first power should be divided by a factor of λ and those to the second power should be divided by a factor of λ^2. To exactly cancel out the effect of an increase in the radical concentration, the scale factor λ should be equal to the system size corresponding to the state when the system has exactly two radicals divided by the actual system size used.

For a homopolymerization system, eq 7a gives the exact value of $N_{tot,min}$ that corresponds to two radicals in the system, so the determination of λ is straightforward. However, for other polymerization systems, eq 7a or its extension can give only an upper bound; therefore, a prerequisite for determining the scale factor is calculating the *exact* minimal system size. For this purpose, we cannot simply use the maximal termination rate coefficient as in eq 7b. Instead, the closed form for the effective termination rate constant must be obtained. To start, the termination rate is written explicitly as a sum of all the different types of termination reaction rates. Then, by factoring out the square of the total number of radicals, the remaining part is the effective termination rate constant.

$$\begin{aligned} k_i C_i &= \sum_{j,k,l,m\in\{1,2\}} k_{t,jk,lm} C_{r,jk} C_{r,lm} \\ &= \sum_{j,k,l,m\in\{1,2\}} \frac{k_{t,jk,lm} C_{r,jk} C_{r,lm}}{C_r^2} C_r^2 \\ &= \left(\sum_{j,k,l,m\in\{1,2\}} k_{t,jk,lm} \frac{C_{r,jk}}{C_r} \frac{C_{r,lm}}{C_r} \right) C_r^2 \end{aligned} \tag{12}$$

where $k_{t,jk,lm}$ is the rate coefficient of termination of two radicals ending with monomers j, k and l, m, respectively. $C_{r,jk}$ is the concentration of radicals with the last two units being monomers j and k.

Equation 12 shows that the effective termination rate constant is a weighted sum of all termination rates, where the weighting factor is the probability of picking two radicals of the corresponding types from all the radicals. This also indicates that in order to calculate the effective termination rate constant, radical fractions need to be calculated.

Radical fractions are calculated by applying the PSSA to each type of radical separately. This is illustrated in eqs 13−16. By solving these equations, the radical fractions can be expressed in terms of the monomer concentration and propagation rate constants. This is shown in eqs 17−20. By substituting these into eq 12, the effective termination rate constant, and thus the exact minimal system size, can be calculated.

$$\frac{dC_{r,11}}{dt} = k_{211} C_{r,21} C_{M_1} - k_{112} C_{r,11} C_{M_2} = 0 \tag{13}$$

$$\frac{dC_{r,12}}{dt} = -k_{121} C_{r,12} C_{M_1} + k_{112} C_{r,11} C_{M_2} - k_{122} C_{r,12} C_{M_2} + k_{212} C_{r,21} C_{M_2} = 0 \tag{14}$$

$$\frac{dC_{r,21}}{dt} = -k_{211} C_{r,21} C_{M_1} + k_{121} C_{r,12} C_{M_1} + k_{221} C_{r,22} C_{M_1} - k_{212} C_{r,21} C_{M_2} = 0 \tag{15}$$

$$\frac{dC_{r,22}}{dt} = -k_{221} C_{r,22} C_{M_1} + k_{122} C_{r,12} C_{M_2} = 0 \tag{16}$$

$$\frac{C_{r,11}}{C_r} = \frac{(k_{121} C_{M_1} + k_{122} C_{M_2}) \frac{k_{211} C_{M_1}}{k_{112} C_{M_2}}}{\Sigma} \tag{17}$$

$$\frac{C_{r,12}}{C_r} = \frac{(k_{211} C_{M_1} + k_{212} C_{M_2})}{\Sigma} \tag{18}$$

$$\frac{C_{r,21}}{C_r} = \frac{(k_{121} C_{M_1} + k_{122} C_{M_2})}{\Sigma} \tag{19}$$

$$\frac{C_{r,22}}{C_r} = \frac{(k_{211} C_{M_1} + k_{212} C_{M_2}) \frac{k_{122} C_{M_2}}{k_{221} C_{M_1}}}{\Sigma} \tag{20}$$

$$\Sigma = (k_{121} C_{M_1} + k_{122} C_{M_2}) \frac{k_{211} C_{M_1}}{k_{112} C_{M_2}} + (k_{211} C_{M_1} + k_{212} C_{M_2}) + (k_{121} C_{M_1} + k_{122} C_{M_2}) + (k_{211} C_{M_1} + k_{212} C_{M_2}) \frac{k_{122} C_{M_2}}{k_{221} C_{M_1}} \tag{21}$$

where k_{ijk} is the propagation rate coefficient for a radical with the last two units being i and j adding a new monomer k, and C_{M_i} is the concentration of monomer i.

A summary of the steps required to scale the rate constants is given below:

(1) Calculate the radical fractions based on monomer composition.

(2) Calculate the effective rate constant using eq 12.

(3) Calculate the exact minimal system size using eq 7b, using effective termination rate constant instead of maximal termination rate constant, rewritten here as

$$N_{tot,exactmin} \le 2 \sqrt{\frac{k_{t,eff}}{k_i C_i}} \left(\sum_{j\in monomers,solvent} \frac{x_j}{\rho_j} \right)^{-1} \tag{7e}$$

(4) Determine the scale factor, λ, which is equal to the exact minimal system size divided by the actual system size used.

In the context of this paper, the term "minimal system size" refers to the number calculated from eq 7b and "exact minimal system size" refers to the number calculated from eq 7e.

It can be seen from the procedure above that the scale factor needs to be updated over the course of polymerization. This, however, only adds a small amount of computational overhead because the updates of the scale factor are far less frequent than the updates of the rates, as will be shown in one of the case studies below. It is also worth pointing out that although eq 12 uses a specific assumption for representing termination rate constants (i.e., depends on the radical type but not chain length), the scaling approach is not limited to this representation and can be applied regardless of how the effective termination rate constant is obtained.

4. CASE STUDIES

4.1. Case 1: Free Radical Polymerization of Butyl Acrylate/Methyl Methacrylate. Butyl acrylate/methyl methacrylate (BA/MMA) copolymerization has been extensively studied, and all kinetic parameters are available in the literature. For this case study, the initial concentration of BA and MMA is

DOI: 10.1021/acs.iecr.5b03198
Ind. Eng. Chem. Res. 2015, 54, 11975−11985

3 mol/L in total, with a 55/45 molar compositional ratio. Benzene is used as the solvent and azodiisobutyronitrile (AIBN) as the initiator. The simulation is carried out at 50 °C. Table 2 lists the physical properties and kinetic parameters used in this calculation.

Table 2. Physical Properties and Rate Constants Used for FRP of BA/MMA

Physical Properties		
molar density (mol/L)	BA	7.01
	MMA	9.40
	benzene (solvent)	11.23
Rate Constants, in Arrhenius Form		
	A (s^{-1} (initiation) or L mol^{-1} s^{-1} (otherwise))	E_a (kcal/mol)
initiation (efficiency f = 0.5)	6.04×10^{15}	31.46
BA homopolymerization	2.21×10^{7}	4.28
MMA homopolymerization	2.67×10^{6}	5.35
BA termination by recombination[a]	3.70×10^{9}	2.01
MMA termination by recombination	1.20×10^{8}	1.34
Reactivity Ratios		
r_1 (k_{111}/ k_{112}, k_{211}/ k_{212})	0.35	
r_2 (k_{222}/ k_{221}, k_{122}/ k_{121})	2.06	
s_1 (k_{111}/ k_{211})	0.40	
s_2 (k_{222}/ k_{122})	1.78	

[a]The fraction of disproportionation to total termination (i.e., disproportionation and recombination) for BA, k_{dis}/k_t = 0.05 and for MMA, k_{dis}/k_t = 0.6. The rate constant of cross-termination is the geometric mean of the homotermination rate coefficients for BA and MMA.

4.1.1. System Behavior with Insufficient System Size. Figure 1 shows a series of conversion versus time profiles with

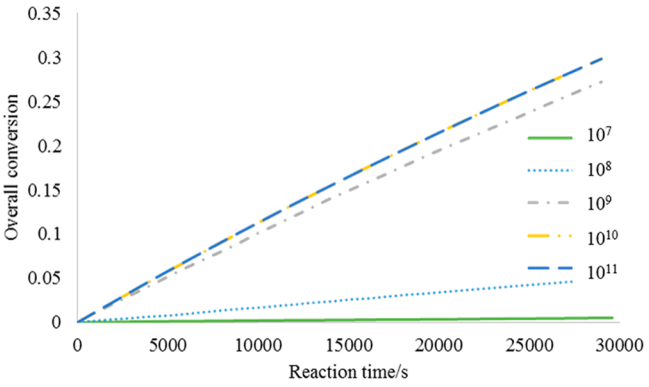

Figure 1. Conversion profiles for different system sizes for BA/MMA copolymerization at 50 °C with BA/MMA = 55/45.

the system size being 10^7, 10^8, 10^9, 10^{10}, or 10^{11}. While the last three cases cannot be differentiated by observation, the first two cases show much lower conversion, which indicates that KMC does not converge until the system size is above 10^9 initial monomers. A more comprehensive comparison of number-average molecular weight, reaction events per molecule, and fractions of different reaction types is listed in Table 3.

It can be seen that for system sizes of 10^7 and 10^8, the number-average molecular weight is much lower than the converged cases. This is consistent with the previous argument that an insufficient system size causes early termination of chains and ultimately produces lower molecular weight. The comparison of reaction events per molecule shows that for system sizes of 10^7 and 10^8 there are fewer reaction events occurring. Also, the proportion of termination and initiation events increases compared to propagation. Overall, each of these results presented here support the previous analyses.

4.1.2. Mathematical Scaling of the Rate Constants. Following the procedure laid out above, radical fractions were calculated based on initial monomer compositions using eqs 17−20 and are listed in Table 4. These radical fractions were used in eq 12 for the calculation of the effective termination rate constant and then the exact minimal system size. The result is 1.39×10^9.

A KMC simulation run using the exact minimal size calculated above generates the explicit distribution of the number of radicals as a function of reaction time, so the average termination rate can be calculated. For copolymerization, because termination can occur both between different radicals and between the same type of radical, the average termination rate needs be explicitly calculated using eq 12, based on the exact type and number of radicals throughout the entire reaction process. The expressions for calculating the average number of radicals and average termination rate are

$$\overline{N_r} = \frac{\int_{t_1}^{t_2} N_r \, dt}{t_2 - t_1} \tag{22}$$

$$\overline{R_t} = \frac{\int_{t_1}^{t_2} R_t dt}{t_2 - t_1} \tag{23}$$

To analyze these quantities, five 1000 s time periods were chosen, and the average number of radicals $\overline{N_r}$ and average termination rate $\overline{R_t}$ were calculated. We also determined the average number of radicals using a continuum expression, calculated as the square root of the average termination rate divided by the effective termination rate constant. Results are listed in Table 5. The effective termination rate constant is divided by VN_A based on the relationship between stochastic and continuum rates.[1] For all time periods, the average number of radicals is approximately 2, indicating that eq 7e predicts the exact minimal system size precisely. Also, the actual average number of radicals is close to the number calculated from the continuum expression, showing the validity of using a continuum model in the development of the scaling relationships and the minimal system size.

To demonstrate the scaling method, two smaller system sizes, 10^7 and 10^8, were selected to test the scaling process. Based on the analysis above, scale factors of 139 and 13.9 were employed for the 10^7 and 10^8 systems, respectively. Figures 2−5 compare the conversion profiles, dyad fractions, and molecular weight distributions for using the exact minimal system size, as well as system sizes of 10^7, 10^8, and 10^{10}. A dyad is two adjacent units in a sequence, which, in the context of copolymerization, can have four configurations: “aa”, “ab”, “ba”, and “bb” (where “a” and “b” represent the two types of monomers). In the cases with insufficient system size, the simulations are carried out with scaled rate constants. The conversion profiles and dyad fractions are virtually indistinguishable among the four cases. For the number-average molecular weight, the first three cases match each other well,

DOI: 10.1021/acs.iecr.5b03198
Ind. Eng. Chem. Res. 2015, 54, 11975−11985

Table 3. Comparison of Number Average Molecular Weight (M_n), Weight Average Molecular Weight (M_w), Polydispersity Index (PDI), Reaction Events Per Molecule and Fractions of Different Types of Reactions for BA/MMA Copolymerization at 50°C with BA/MMA = 55/45 at 3×10^4 s

system size	10^7	10^8	10^9	10^{10}	10^{11}
M_n (g/mol)	4.56×10^3	4.53×10^4	2.53×10^5	2.80×10^5	2.81×10^5
M_w (g/mol)	8.46×10^3	1.04×10^4	5.70×10^5	5.50×10^5	5.40×10^5
PDI	1.86	2.29	2.25	1.96	1.92
total number of reaction events/system size $\times 10^3$	1.50	15.2	84.3	92.5	92.6
percentage of initiation reactions	7.35	0.76	0.14	0.13	0.13
percentage of termination reactions	1.47	0.15	0.03	0.02	0.02
percentage of propagation reactions	91.18	99.08	99.83	99.85	99.85

Table 4. Radical Fractions Based on Initial Monomer Compositions

radical type	$P^{\bullet}_{11}$	$P^{\bullet}_{12}$	$P^{\bullet}_{21}$	$P^{\bullet}_{22}$
fraction	0.0016	0.2459	0.0096	0.7428

Table 5. Frequency of Observing Different Numbers of Radicals and the Average Value

reaction time period (s)	$\overline{N_r}$	$\overline{R_t}$ (mol L^{-1} s^{-1})	$\left(\frac{\overline{R_t}}{k_{t,eff}/VN_A}\right)^{1/2}$
1000−2000	1.96	1.14	2.07
2000−3000	1.98	1.12	2.05
3000−4000	1.96	1.10	2.03
4000−5000	2.04	1.15	2.08
5000−6000	2.00	1.12	2.05

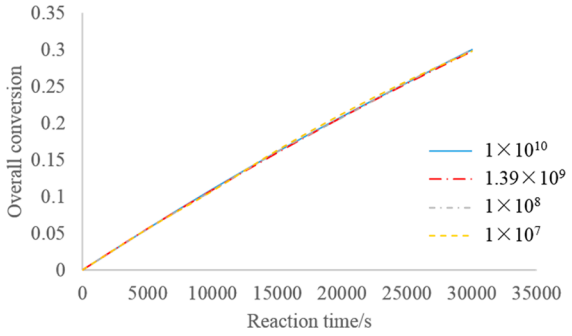

Figure 2. Comparison of conversion between four cases with system sizes of 10^{10}, 1.39×10^9 (exact minimal system size), 10^8, and 10^7, with the last two cases using scaled rate constants.

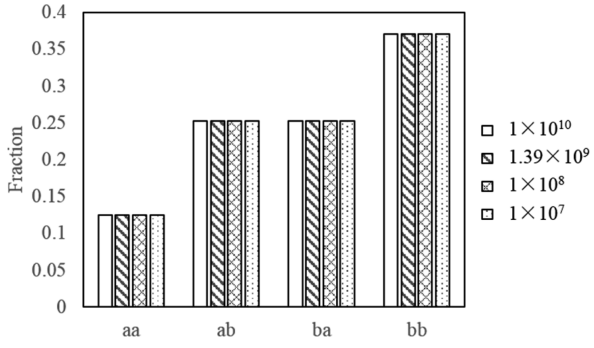

Figure 3. Comparison of dyad fractions for a reaction time of 3×10^4 s among four cases with system sizes of 10^{10}, 1.39×10^9 (exact minimal system size), 10^8, and 10^7, with the last two cases using scaled rate constants.

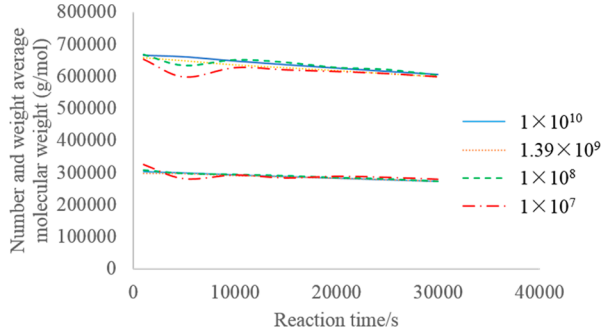

Figure 4. Comparison of number and weight-average molecular weight among four cases with system sizes of 10^{10}, 1.39×10^9 (exact minimal system size), 10^8, and 10^7, with the last two cases using scaled rate constants.

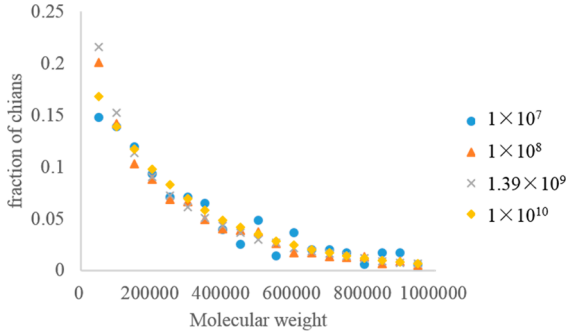

Figure 5. Comparison of the full molecular weight distribution at 3×10^4 s among four cases with system sizes of 10^{10}, 1.39×10^9 (exact minimal system size), 10^8, and 10^7, with the last two cases using scaled rate constants.

while it requires a discernible period of time for the last case (10^7 scaled) to converge to the same result. This is because, at the early stage of the reaction, the number of polymer chains generated is significantly smaller. The comparison in Figure 5 further demonstrates that the molecular weight distribution does not deviate from the correct result when the system size is reduced and scaling is incorporated. Therefore, it can be concluded that the scaling of the rate constants makes it possible to maintain converged results with system sizes more than 100 times smaller than the minimum. This acceleration is comparable to that achieved using the hybrid approach proposed by Tripathi and Sundberg.[13] Moreover, these two approaches have the potential to be combined and achieve further acceleration, which is currently being explored.

The clear value of this scaling approach is demonstrated by comparing the time required for the simulations with different system sizes for a total reaction time of 3×10^4 s. Table 6

DOI: 10.1021/acs.iecr.5b03198
Ind. Eng. Chem. Res. 2015, 54, 11975−11985

Table 6. Comparison of Various Measures of Simulation Time and Number of KMC Events for Scaled and Unscaled Cases for a Total Reaction Time of 3×10^4 s[a]

		10^7	10^8	1.39×10^9	10^{10}
total simulation time (s)	unscaled	*0.02*	*2.26*	193	1375
	scaled	1.79	18.5	NA	NA
number of KMC events	unscaled	*1.50×10^4*	*1.52×10^6*	1.27×10^8	9.25×10^8
	scaled	9.25×10^5	9.18×10^6	NA	NA
simulation time (s)/ system size $\times 10^7$	unscaled	*0.02*	*0.226*	1.38	1.375
	scaled	1.79	1.85	NA	NA
simulation time (s)/ KMC event $\times 10^6$	unscaled	*1.33*	*1.49*	1.52	1.49
	scaled	1.93	1.85	NA	NA

[a]Note that the correct results (e.g., conversion, molecular weight) for the unscaled cases with system sizes of 10^7 and 10^8 are not obtained; thus, the total simulation times appear low. These entries are indicated in italics to underscore this point.

shows the number of KMC events and various measures of simulation time for these four cases, comparing between the scaled and unscaled cases. With the scaling method implemented, the number of KMC events remains proportional to the system size. We also divided simulation time by the system size, revealing that scaling does introduce a small amount of extra overhead on a per molecule basis, but overall the time savings is dramatic. To achieve results that are in very good agreement, the scaled 10^7 case provides an acceleration of 2 orders of magnitude compared to the minimal system size case.

However, this system size reduction is not unlimited. When the system size becomes increasingly small, the number of polymer chains will become too small to avoid random effects, and results will show stochastic fluctuations with repeated runs under the same conditions, as shown in Figure 6 for the molecular weight profiles for 10 repeated runs with 10^6 system size. When the results of these 10 runs are averaged, it resembles the case with 10^7 molecules. A certain transition period is needed, but the profile finally converges to the expected result (Figure 7). If parallelization techniques are used, running 10 simulations using 10^6 molecules would result in a smaller wall time than a single run of 10^7 molecules. However, the chain information would be averaged, losing the full range of explicit sequence information encoded in the set of chains from 10 explicit runs equal in number to the 10^7 case.

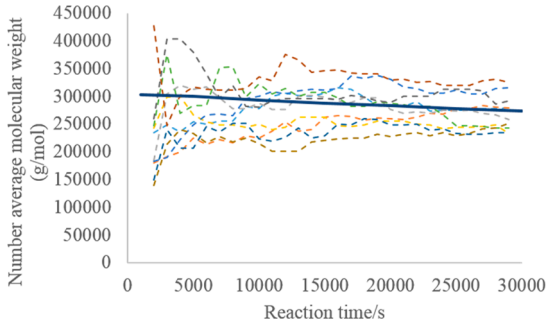

Figure 6. Number-average molecular weight profiles for 10 repeated runs with 10^6 system size (dashed lines), even when scaled rate coefficients are incorporated, compared with the converged result (solid line, using 10^{10} molecules).

4.2. Case 2: Methyl Acrylate/MMA Copolymerization. This case study applies the proposed method to a methyl acrylate (MA)/MMA copolymerization system, using different synthesis conditions. The kinetic parameters used in this case study are shown in Table 7. This case uses an initiator concentration of 0.015 mol/L and a monomer molar composition of 30/70, both significantly different from the prior BA/MMA case. The total molar concentration of monomers is 3 mol/L, and simulations are run at two different temperatures, 50 and 80 °C.

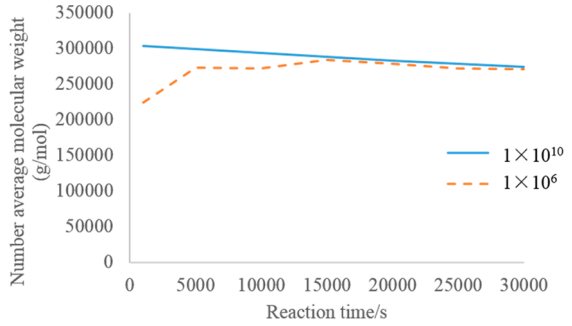

Figure 7. Comparison between the average of the number-average molecular weight profiles of 10 repeated runs using 10^6 molecules with scaled rate coefficients and the result obtained using 10^{10} molecules.

Table 7. Physical Properties and Rate Constants Used for FRP of MA/MMA

Physical Properties		
molar density (mol/L)	MA	11.05
	MMA	9.40
	benzene (solvent)	11.23
Rate Constants, in Arrhenius Form		
	A (s^{-1} (initiation) or L mol^{-1} s^{-1} (otherwise))	E_a (kcal/mol)
initiation (efficiency $f = 0.5$)	6.04×10^{15}	31.46
MA homopolymerization	6.90×10^6	3.75
MMA homopolymerization	2.67×10^6	5.35
MA termination by recombination[a]	3.02×10^9	2.08
MMA termination by recombination	1.20×10^8	1.34
Reactivity Ratios		
r_1 (k_{111}/ k_{112}, k_{211}/ k_{212})	0.42	
r_2 (k_{222}/ k_{221}, k_{122}/ k_{121})	2.36	
s_1 (k_{111}/ k_{211})	0.40	
s_2 (k_{222}/ k_{122})	1.78	

[a]The fraction of disproportionation to total termination (i.e., disproportionation and recombination) for MA, $k_{dis}/k_t = 0.05$, and for MMA, $k_{dis}/k_t = 0.6$. The rate constant of cross-termination is the geometric mean of the homotermination ones for MA and MMA

DOI: 10.1021/acs.iecr.5b03198
Ind. Eng. Chem. Res. 2015, 54, 11975−11985

The exact minimal system size is calculated to be 8.69×10^8 and 1.19×10^8 for temperatures equal to 50 and 80 °C, respectively. For each temperature, one system size above the exact minimal and two smaller system sizes are simulated. Conversion profiles, molecular weight profiles, and dyad fractions are compared for different system sizes, with the rate coefficients being properly scaled for cases with insufficient system size. Results are shown in Figures 8–10. In Figure 10,

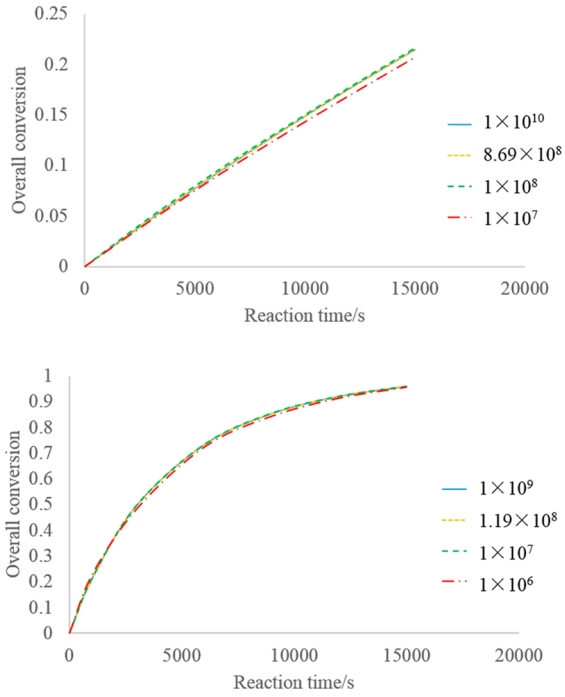

Figure 8. Conversion profiles for MA/MMA polymerization at 50 °C (upper panel) and 80 °C (lower panel) for different system sizes. For system sizes of 10^7 and 10^8 (upper panel) or 10^6 and 10^7 (lower panel), scaled rate coefficients were used.

the upper four curves represent weight-average molecular weight and the lower four curves represent number-average molecular weight. As was observed for BA/MMA polymerization, the largest deviation occurs for weight-average molecular weight with small system sizes, when a single chain can have a relatively strong impact on the population average. Despite this, the differences are reasonably small so that it can be concluded that all simulated properties show good agreement between different system sizes, and the computational time gains (not shown) are similar to those observed for the BA/MMA system. It should also be noted that for the 80 °C case, the initiator half-life is short compared to the reaction time, so there is a significant decrease in radical concentration over the course of the reaction. This case study demonstrates the general applicability of the scaling approach under different scenarios.

For all the cases explored above, the reduction of the system size enabled by rate constant scaling can reduce the number of molecules by 2 orders of magnitude. Along with the system size, the number of polymer chains generated decreases by a factor of 100, while still matching key quantities such as conversion, molecular weight, and dyad fractions. This sample of polymeric chains is a good representation of the larger chain population and can potentially be useful as an input for

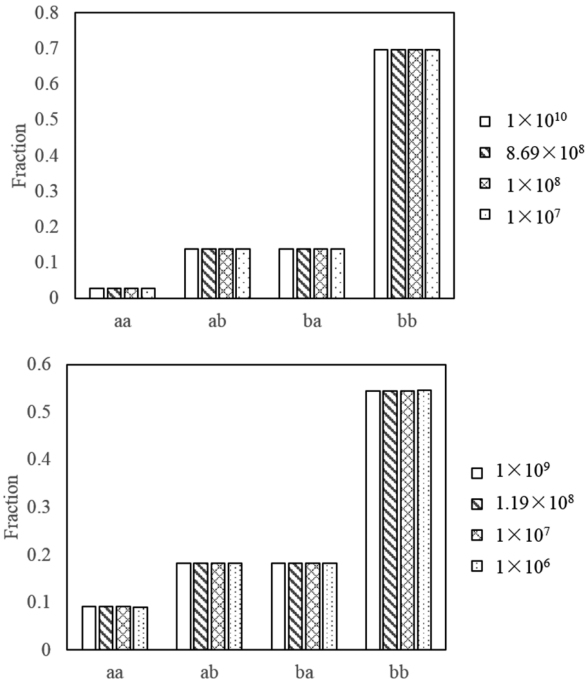

Figure 9. Dyad fractions at reaction time of 15 000 s for MA/MMA polymerization at 50 °C (upper panel) and 80 °C (lower panel) for different system sizes. For system sizes of 10^7 and 10^8 (upper panel) or 10^6 and 10^7 (lower panel), scaled rate coefficients were used.

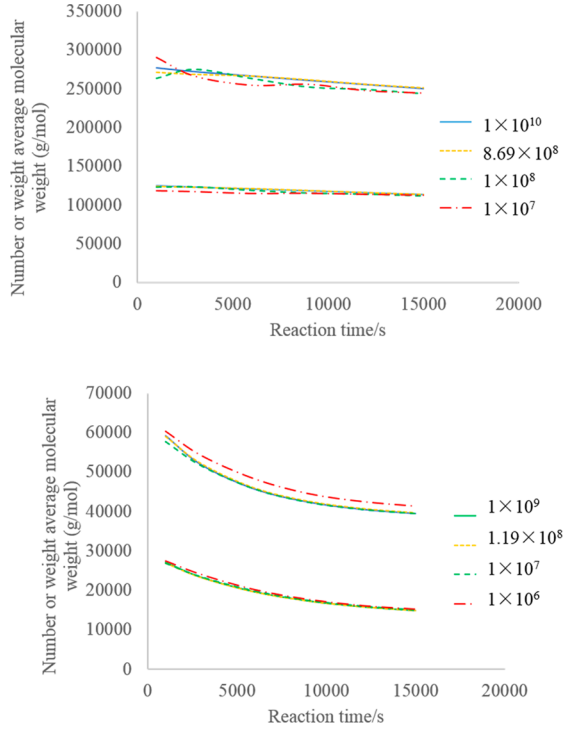

Figure 10. Number-average and weight-average molecular weight profiles for MA/MMA polymerization at 50 °C (upper panel) and 80 °C (lower panel) for different system sizes. For system sizes of 10^7 and 10^8 (upper panel) or 10^6 and 10^7 (lower panel), scaled rate coefficients were used.

molecular simulation, thereby enabling a multiscale modeling approach to study polymeric systems.

DOI: 10.1021/acs.iecr.5b03198
Ind. Eng. Chem. Res. 2015, 54, 11975–11985

5. CONCLUSION

The minimal system size for KMC simulations of free radical polymerization processes can be determined based on synthesis conditions. This approach was generalized to more complicated free radical reaction systems by simplifying the initiation reaction channels. By properly scaling the rate constants, the system size was further reduced, accelerating simulations by 2 orders of magnitude and generating a smaller sample of polymer chains representative of the chain population associated with the KMC simulation when the number of molecules in the system equaled or exceeded the necessary minimum value. Furthermore, this work may facilitate the linkage of KMC output with molecular simulations to explore structure−property relationships such as chain sequence and physical properties, such as glass transition temperature and mass transport properties, because molecular simulation can handle only a limited number of molecules. This can be an important step toward formulating a multiscale model.

■ ASSOCIATED CONTENT

Supporting Information

The Supporting Information is available free of charge on the ACS Publications website at DOI: 10.1021/acs.iecr.5b03198.

Reaction mechanism of autoxidative crosslinking (PDF)

■ AUTHOR INFORMATION

Corresponding Author

*E-mail: broadbelt@northwestern.edu.

Notes

The authors declare no competing financial interest.

■ ACKNOWLEDGMENTS

The work is supported by The Dow Chemical Company. Financial support from the National Science Foundation (DMR-1241667) is also gratefully acknowledged.

■ REFERENCES

(1) Gillespie, D. T. A general method for numerically simulating the stochastic time evolution of coupled chemical reactions. *J. Comput. Phys.* **1976**, *22*, 403−434.

(2) Bujak, P.; Matlengiewicz, M.; Pasich, M.; Henzel, N. Microstructure of methyl methacrylate/tert-butyl acrylate copolymer characterized by ^{13}C NMR spectroscopy. *Polym. Bull.* **2010**, *64* (3), 259−273.

(3) Huijser, S.; Staal, B. B.; Huang, J.; Duchateau, R.; Koning, C. E. Chemical composition and topology of poly(lactide-co-glycolide) revealed by pushing MALDI-TOF MS to its limit. *Angew. Chem., Int. Ed.* **2006**, *45* (25), 4104−4108.

(4) Kitayama, T.; Ute, K.; Hatada, K. Synthesis of stereoregular polymers and copolymers of methacrylate by living polymerization and their characterization by NMR-spectroscopy. *Br. Polym. J.* **1990**, *23* (1−2), 5−17.

(5) Koening, L. *Chemical Microstructure of Polymer Chains*; Wiley-Interscience: New York, 1980.

(6) Nguyen, G.; Nicole, D.; Matlengiewicz, M.; Roizard, D.; Henzel, N. Relation between microstructure and glass transition temperature of poly[(methyl methacrylate)-co-(ethyl acrylate)]. *Polym. Int.* **2001**, *50* (7), 784−791.

(7) Wulkow, M. Computer aided modeling of polymer reaction engineering-the status of Predici, 1-simulation. *Macromol. React. Eng.* **2008**, *2* (6), 461−494.

(8) Vinu, R.; Broadbelt, L. J. Unraveling reaction pathways and specifying reaction kinetics for complex systems. *Annu. Rev. Chem. Biomol. Eng.* **2012**, *3*, 29−54.

(9) Meimaroglou, D.; Kiparissides, C. A novel stochastic approach for the prediction of the exact topological characteristics and rheological properties of highly-branched polymer chains. *Macromolecules* **2010**, *43* (13), 5820−5832.

(10) Sosnowski, S. Software for demonstration of features of chain polymerization processes. *J. Chem. Educ.* **2013**, *90* (6), 793−795.

(11) Van Steenberge, P. H. M.; D'hooge, D. R.; Reyniers, M. F.; Marin, G. B. Improved kinetic Monte Carlo simulation of chemical composition-chain length distributions in polymerization processes. *Chem. Eng. Sci.* **2014**, *110*, 185−199.

(12) Regatte, V. R.; Gao, H.; Konstantinov, I. A.; Arturo, S. G.; Broadbelt, L. J. Design of copolymers based on sequence distribution for a targeted molecular weight and conversion. *Macromol. Theory Simul.* **2014**, *23* (9), 564−574.

(13) Tripathi, A. K.; Sundberg, D. C. A hybrid algorithm for accurate and efficient Monte Carlo simulations of free-radical polymerization reactions. *Macromol. Theory Simul.* **2015**, *24* (1), 52−64.

(14) Van Steenberge, P. H. M.; D'hooge, D. R.; Wang, Y.; Zhong, M.; Reyniers, M.-F.; Konkolewicz, D.; Matyjaszewski, K.; Marin, G. B. Linear gradient quality of ATRP copolymers. *Macromolecules* **2012**, *45* (21), 8519−8531.

(15) Van Steenberge, P. H. M.; Vandenbergh, J.; D'hooge, D. R.; Reyniers, M.-F.; Adriaensens, P. J.; Lutsen, L.; Vanderzande, D. J. M.; Marin, G. B. Kinetic Monte Carlo modeling of the sulfinyl precursor route for poly(p-phenylene vinylene) synthesis. *Macromolecules* **2011**, *44* (22), 8716−8726.

(16) Wang, L.; Broadbelt, L. J. Tracking explicit chain sequence in kinetic Monte Carlo simulations. *Macromol. Theory Simul.* **2011**, *20* (1), 54−64.

(17) Wang, L.; Broadbelt, L. J. Explicit sequence of styrene/methyl methacrylate gradient copolymers synthesized by forced gradient copolymerization with nitroxide-mediated controlled radical polymerization. *Macromolecules* **2009**, *42* (20), 7961−7968.

(18) Drache, M.; Schmidt-Naake, G.; Buback, M.; Vana, P. Modeling RAFT polymerization kinetics via Monte Carlo methods: cumyl dithiobenzoate mediated methyl acrylate polymerization. *Polymer* **2005**, *46* (19), 8483−8493.

(19) Al-Harthi, M.; Soares, J. B.; Simon, L. C. Dynamic Monte Carlo simulation of atom-transfer radical polymerization. *Macromol. Mater. Eng.* **2006**, *291* (8), 993−1003.

(20) Mohammadi, Y.; Najafi, M.; Haddadi-Asl, V. Comprehensive study of free radical copolymerization using a Monte Carlo simulation method, 1. *Macromol. Theory Simul.* **2005**, *14* (5), 325−336.

(21) Najafi, M.; Haddadi-Asl, V.; Mohammadi, Y. Application of the Monte Carlo simulation method to the investigation of peculiar free-radical copolymerization reactions: Systems with both reactivity ratios greater than unity ($r_A > 1$ and $r_B > 1$). *J. Appl. Polym. Sci.* **2007**, *106* (6), 4138−4147.

(22) Brandão, A. L.; Soares, J. B.; Pinto, J. C.; Alberton, A. L. When polymer reaction engineers play dice: Applications of Monte Carlo models in PRE. *Macromol. React. Eng.* **2015**, *9* (3), 141−185.

(23) Chaffey-Millar, H.; Stewart, D.; Chakravarty, M. M.; Keller, G.; Barner-Kowollik, C. A parallelised high performance Monte Carlo simulation approach for complex polymerisation kinetics. *Macromol. Theory Simul.* **2007**, *16* (6), 575−592.

(24) Lemos, T.; Melo, P. A.; Pinto, J. C. Stochastic modeling of polymer microstructure from residence time distribution. *Macromol. React. Eng.* **2015**, *9* (3), 259−270.

(25) Iedema, P. D.; Hoefsloot, H. C. Synthesis of branched polymer architectures from molecular weight and branching distributions for radical polymerisation with long-chain branching, accounting for topology-controlled random scission. *Macromol. Theory Simul.* **2001**, *10* (9), 855−869.

(26) Iedema, P. D.; Hoefsloot, H. C. Predicting molecular weight and degree of branching distribution of polyethylene for mixed systems with a constrained geometry metallocene catalyst in semibatch and continuous reactors. *Macromolecules* **2003**, *36* (17), 6632−6644.

DOI: 10.1021/acs.iecr.5b03198
Ind. Eng. Chem. Res. 2015, 54, 11975−11985

(27) Lagache, M.; Ungerer, P.; Boutin, A.; Fuchs, A. Prediction of thermodynamic derivative properties of fluids by Monte Carlo simulation. *Phys. Chem. Chem. Phys.* **2001**, *3* (19), 4333−4339.
(28) Shah, J. K.; Brennecke, J. F.; Maginn, E. J. Thermodynamic properties of the ionic liquid 1-n-butyl-3-methylimidazolium hexafluorophosphate from Monte Carlo simulations. *Green Chem.* **2002**, *4* (2), 112−118.
(29) Rane, K. S.; Murali, S.; Errington, J. R. Monte Carlo simulation methods for computing liquid−vapor saturation properties of model systems. *J. Chem. Theory Comput.* **2013**, *9* (6), 2552−2566.
(30) Ali Parsa, M.; Kozhan, I.; Wulkow, M.; Hutchinson, R. A. Modeling of functional group distribution in copolymerization: A comparison of deterministic and stochastic approaches. *Macromol. Theory Simul.* **2014**, *23* (3), 207−217.
(31) Gillespie, D. T. Stochastic simulation of chemical kinetics. *Annu. Rev. Phys. Chem.* **2007**, *58*, 35−55.
(32) Odian, G. *Principles of Polymerization*; John Wiley & Sons: Hoboken, NJ, 2004.
(33) Burke, A. L.; Duever, T. A.; Penlidis, A. Model discrimination via designed experiments - discrimination between the terminal and penultimate models based on rate data. *Chem. Eng. Sci.* **1995**, *50* (10), 1619−1634.
(34) Fukuda, T.; Ma, Y. D.; Inagaki, H. Free-radical copolymerization 0.3. Determination of rate constants of propagation and termination for the styrene methyl-methacrylate system - a critical test of terminal-model kinetics. *Macromolecules* **1985**, *18* (1), 17−26.
(35) Madruga, E. L.; Fernández-García, M. A kinetic study of free-radical copolymerization of butyl acrylate with methyl methacrylate in solution. *Macromol. Chem. Phys.* **1996**, *197* (11), 3743−3755.
(36) Liu, S.-l.; Amundson, N. R. Analysis of Polymerization kinetics and the use of a digital computer. *Rubber Chem. Technol.* **1961**, *34* (4), 995−1133.
(37) Spade, C. A.; Volpert, V. A. On the steady-state approximation in thermal free radical frontal polymerization. *Chem. Eng. Sci.* **2000**, *55* (3), 641−654.
(38) Kiss, A. A.; Bildea, C. S.; Dimian, A. C.; Iedema, P. D. State multiplicity in CSTR−separator−recycle polymerisation systems. *Chem. Eng. Sci.* **2002**, *57* (4), 535−546.
(39) Šebenik, U.; Krajnc, M. Seeded semibatch emulsion copolymerization of methyl methacrylate and butyl acrylate using polyurethane dispersion: Effect of soft segment length on kinetics. *Colloids Surf., A* **2004**, *233* (1), 51−62.
(40) Hamielec, A.; Hodgins, J.; Tebbens, K. Polymer reactors and molecular weight distribution: Part II. Free radical polymerization in a batch reactor. *AIChE J.* **1967**, *13* (6), 1087−1091.
(41) Verros, G. D.; Latsos, T.; Achilias, D. S. Development of a unified framework for calculating molecular weight distribution in diffusion controlled free radical bulk homo-polymerization. *Polymer* **2005**, *46* (2), 539−552.
(42) Shojaei, A.; Ghaffarian, S.; Karimian, S. Numerical simulation of three-dimensional mold filling process in resin transfer molding using quasi-steady state and partial saturation formulations. *Compos. Sci. Technol.* **2002**, *62* (6), 861−879.
(43) Verros, G. D. Calculation of molecular weight distribution in non-linear free radical copolymerization. *Polymer* **2003**, *44* (22), 7021−7032.
(44) Szymanski, R. On the incorrectness of the factor 2 in the radical termination equation. *Macromol. Theory Simul.* **2011**, *20* (1), 8−12.
(45) Learner, T. *Analysis of modern paints*; Getty Conservation Institute: Los Angeles, 2004.
(46) Van Gorkum, R.; Bouwman, E. The oxidative drying of alkyd paint catalysed by metal complexes. *Coord. Chem. Rev.* **2005**, *249* (17), 1709−1728.
(47) Bouwman, E.; Van Gorkum, R. A study of new manganese complexes as potential driers for alkyd paints. *Journal of Coatings Technology and Research* **2007**, *4* (4), 491−503.
(48) Ploeger, R.; Scalarone, D.; Chiantore, O. The characterization of commercial artists' alkyd paints. *Journal of Cultural Heritage* **2008**, *9* (4), 412−419.

DOI: 10.1021/acs.iecr.5b03198
Ind. Eng. Chem. Res. 2015, 54, 11975−11985